

# Predicting the robust features of the out-of-equilibrium evolution of many-body quantum systems

J. Surace and M. Piani

*Department of Physics and SUPA, University of Strathclyde, Glasgow G4 0NG, United Kingdom*

L. Tagliacozzo

*Department of Physics and SUPA, University of Strathclyde, Glasgow G4 0NG, United Kingdom and  
Departament de Física Quàntica i Astrofísica and Institut de Ciències del Cosmos (ICCUB),  
Universitat de Barcelona, Martí i Franquès 1, 08028 Barcelona, Catalonia, Spain*

The fact that the computational cost of simulating a many-body quantum system on a computer increases with the amount of entanglement has been considered as the major bottleneck for simulating its out-of-equilibrium dynamics. Some aspects of the dynamics are, nevertheless, robust under appropriately devised approximations. Here we present a possible algorithm that allows to systematically approximate the equilibration value of local operators after a quantum quench. At the core of our proposal there is the idea to transform entanglement between distant parts of the system into mixture, and at the same time preserving those conserved quantities that can be expressed as a sum of local densities. We benchmark the resulting algorithm by studying quenches of quadratic fermionic Hamiltonians.

## I. INTRODUCTION

Simulating the time evolution of many-body quantum systems by classical means is hard. In fact, simulating an  $N$  constituents system requires storage and computation time that scale exponentially with  $N$ . As an example, consider the exponentially large space needed in order to store the  $2^N$  complex coefficients describing the state of a  $\frac{1}{2}$  spin chain of length  $N$ . In some cases the specific structure of the problem allows to devise efficient classical algorithms for simulating many-body systems. For example, in the context of statistical mechanics, a many-body system can have exponentially many configurations. However, in most cases, using Monte-Carlo algorithms, we can sample only a polynomially-large set of those configurations, thus simulating the system efficiently [1].

In the context of many-body quantum systems at equilibrium, the locality of correlations [2–4] can be exploited in order to design efficient algorithms based on tensor networks. The most notable examples are DMRG that, as of today, provides the most accurate results for strongly correlated one-dimensional quantum systems [5, 6] and its higher dimensional generalisations (see e.g. [7, 8]).

The locality of correlations at equilibrium implies that the relevant states only have a limited amount of entanglement [2, 3]. As a result their entanglement grows only proportionally to the boundary of a region rather than its volume, a phenomenon formalised in the “area law” of entanglement [4, 8–10].

The locality of correlations is lost in the context of many-body quantum systems out of equilibrium. Out of equilibrium, initially localised correlations can be radiated to arbitrarily large distances [11, 12] leading to a fast growth of entanglement with time [13–18]. Traditional tensor network approaches thus fail to reproduce

the out-of-equilibrium dynamics at relatively short times [19].

Here we circumvent these difficulties by focusing on reproducing a restricted set of local correlations rather than attacking the simulation of the full many-body quantum system at long times. We show that these correlations are sufficient in order to accurately predict some robust aspects (that we define later) of the long-time evolution of local operators.

The long-time evolution is correctly described on average by the *diagonal ensemble* (DE), whose direct construction is also exponentially hard. Our algorithm thus can be considered as an efficient way to locally approximate the DE. In the generic cases, the DE can be approximated by an appropriately designed Gibbs ensemble as a consequence of the *eigenstate thermalisation hypothesis* (ETH) [20–25].

In that context similar ideas to the ones presented here have already been explored [26, 27]. Here we show that our algorithm works also in the more challenging cases in which the ETH is violated such as the case of exactly solvable models. In those systems, the DE is locally approximated by a Generalized Gibbs ensemble whose computation is also exponentially hard [22, 28–35]. However, for the systems we consider here, truncated version of the Generalized Gibbs ensemble provide very accurate local approximation to the DE [36–39]. We believe this is the ultimate origin of the success of our algorithm.

By working with free-fermionic systems furthermore, we are able to accurately benchmark the effects of the approximation involved in the algorithm against exact results. Our exact results refer both to the full out-of-equilibrium dynamics of the system and to the Gaussian state  $\rho_{GDE}$  (Gaussian diagonal ensemble [40]) built from the symbol matrix  $\Lambda_{DE}$  (5) of the DE. In general this state can be different from the actual diagonal ensemble  $\rho_{DE}$ . However, in the specific case we consider here, the two states coincide locally for finite size sys-

tems. Whenever the two ensemble coincide we will thus refer to the  $\rho_{GDE}$  as  $\rho_{DE}$ . The possible discrepancies between  $\rho_{GDE}$  and  $\rho_{DE}$  have already been largely studied in the literature, e.g.  $\rho_{GDE}$  has been characterised numerically in [28] (where it is called *fully constrained thermodynamic ensemble*) and through the recent analytical calculations presented in [41, 42] (where  $\rho_{GDE}$  is called *Gaussian Generalised Gibbs Ensemble*).

One of the key ingredients of our algorithm is to trade entanglement with mixture, (similarly to the algorithm proposed in [26]) forcing us to work in the context of mixed states.

By working with Gaussian states we can accurately monitor if the approximations that we introduce along the simulations spoil the positivity of the mixed states (a calculation that is impossible in the context of matrix product operators used in [26]). We show that by moderately increasing the computational resources we are able to restore the physicality of the mixed states over increasingly large distances, thus proving that our algorithm can provide a viable approximation to the DE over arbitrarily large regions.

## II. ROBUST ASPECTS OF QUANTUM QUENCHES

In the following we focus on the out-of-equilibrium dynamics after a quantum quench [43]. Initially the system is at equilibrium, say in the ground state  $|\psi\rangle$  of some local Hamiltonian  $H$ . The Hamiltonian is abruptly changed from  $H$  to  $\tilde{H}$ , quenching the system out-of-equilibrium. The corresponding evolution is described by

$$|\psi(t)\rangle = e^{-it\tilde{H}}|\psi\rangle. \quad (1)$$

Cardy and Calabrese [11] showed that in this setting the entanglement entropy between two different partitions of  $|\psi(t)\rangle$  grows linearly in time, a footprint of the radiation of the correlation as pseudo-particles [11, 32, 39, 44, 45]. This leads the corresponding states to become too entangled and hard to represent with standard algorithms after relatively short times [19, 46][47].

The short-time dynamics is highly non-universal and very sensitive to the specific details of the quench [48].

Here we try to address robust features of the out-of-equilibrium dynamics after a quench, that is, features that are not too sensitive to the specific details of the quench. One of such features is the equilibration of local observables occurring at long times after the quench.

In most cases the values of the relaxed local observables are indistinguishable from those computed on the DE defined as

$$\rho_{DE(H)} := \sum_n |E_n\rangle\langle E_n|\rho|E_n\rangle\langle E_n|, \quad (2)$$

where  $\{|E_n\rangle\}_n$  are the eigenvectors of the Hamiltonian  $H$  driving the dynamics and  $\rho$  encodes the state

of the system before the quench. That is, if an observable  $A$  equilibrates, at late times after the quench  $\langle A(t)\rangle \simeq \text{Tr}[A\rho_{DE(H)}]$ .

The DE is locally approximated by a Gibbs ensemble in systems obeying the ETH [20–25]. The temperature of the Gibbs ensemble only depends on the energy of the initial state unveiling a high degree of robustness in the process of thermalization.

Not all the relaxing systems satisfy the ETH, and in general robustness can be harder to observe. In particular, the relaxed state of exactly solvable models, depends not only on the temperature, but on infinitely many parameters. They encode the initial values of all the operators conserved during the dynamics. The equilibration of these systems is known to be locally well approximated by *generalised Gibbs ensemble* (GGE) the state that maximizes the entropy at fixed value of all these conserved quantities [22, 28, 36–39].

The dependence of the equilibrium state on infinitely many parameters seems to completely spoil the robustness of the equilibration process. However, a weaker notion of robustness can be recovered in specific exactly solvable models. We can still locally approximate the GGE using few parameters, thus with a higher degree of robustness. This idea is inspired by the fact that systematic local approximations to the GGE can often be obtained by considering states constructed out of only those conserved quantities with local densities as shown in [36, 37] (see however [49–52] for cases in which this reconstruction is not possible).

We thus aim at constructing an efficient algorithm allowing us to predict the equilibration of local observables by approximating the dynamics while protecting those conserved quantities with local densities. Our algorithm exploits our ability to perform exactly the short time dynamics of a many-body quantum system. Once the complexity of the evolved state exceeds the available computational resources, we trade the exact state with an approximate one that we can encode with the available resources.

The size of the support of the local densities that are protected thus constitute the refinement parameter of the algorithm. The refinement parameter affects both the precision of the computation and the resources required to perform it. When the refinement parameter approaches the size of the system, the dynamics becomes exact.

Our algorithms gets inspiration from the Jayne’s principle [53, 54], at each step the entropy grows but the “relevant” conserved quantities are kept fixed. In the process we avoid to diagonalise the full Hamiltonian [55], something that is un-avoidable if aiming at directly constructing the GGE.

Similar ideas have been pursued in the context of tensor networks [26, 27, 56] for systems that thermalise. Here, by using free fermionic systems we are able to compare the approximated dynamics to the exact one, and analyse issues such as the physicality of the state ob-

tained during the evolution (that cannot be addressed in the context of tensor networks). In this way we can better understand up to which extent the results presented provide a faithful description of a physical system out-of-equilibrium.

### III. THE ALGORITHM

Here we focus on free fermionic systems whose relevant states are Gaussian (see Appendix VI A). As a specific example we will consider the transverse field Ising model

$$H(\theta) = -\sin(\theta) \sum_{i=0}^{N-1} \sigma_i^x \sigma_{i+1}^x - \cos(\theta) \sum_{i=0}^{N-1} \sigma_i^z, \quad (3)$$

that can be re-expressed as a free-fermionic Hamiltonian

$$H(\theta) = -\sin(\theta) \sum_{i=0}^{N-1} \left[ a_i^\dagger a_{i+1} - a_i a_{i+1}^\dagger + a_i^\dagger a_{i+1}^\dagger - a_i a_{i+1} \right] + \\ -\cos(\theta) \sum_{i=0}^{N-1} \left[ a_i^\dagger a_i - a_i a_i^\dagger \right]. \quad (4)$$

Because of the Wick theorem a generic Gaussian state is fully characterised by the two point correlation functions which can be organised in the so called symbol or correlation matrix [57–59]

$$\Lambda_{i,j} = \langle \vec{\alpha}_i \vec{\alpha}_j^\dagger \rangle \quad (5)$$

where  $\vec{\alpha}^\dagger = (a_1, a_2, \dots, a_N, a_1^\dagger, a_2^\dagger, \dots, a_N^\dagger)$  is the collection of annihilation and creations operators for every site.

We study the out-of-equilibrium evolution after a sudden quench. We start from the ground state of the Hamiltonian (4) for a given  $\theta_0$ ,  $H(\theta_0)$ . The ground state is encoded in the correlation matrix  $\Lambda_0$  and we let it evolve with an Hamiltonian having the same structure but defined by different value of  $\theta$ ,  $H(\theta)$ . In this way we quench the system out of equilibrium. The out-of-equilibrium evolution of free-fermionic systems can be computed exactly providing the ideal setting for benchmarking our new approximate algorithm.

In particular we want be able to approximate locally the relaxed state using as little information as possible about the state at each step of the evolution aiming for an efficient algorithm to predict locally the state emerging at long times after the quench.

The approximate algorithm should, i) contain a refinement parameter  $m$  allowing to tune the precision. For small values of  $m$  we only obtain very rough results. They should systematically improve and converge to the exact ones as  $m$  is increased; ii) preserve those conserved quantities expressed as the sum of local enough densities (for example, the energy or the number of particles). The

privileged role of these conserved quantities in the context of the out-of-equilibrium evolution has been widely discussed in the literature [36].

The simplest approximation scheme that fulfils i) and ii) consists in defining a truncated matrix  $T_m(\Lambda)$  with  $m \in [0, \lfloor \frac{N}{2} \rfloor]$  obtained from  $\Lambda$  by setting all the matrix elements corresponding to correlations at distances  $d > m$  to zero. For every finite-size system made by  $N$  constituents, as  $m$  grows to  $m = \lfloor \frac{N}{2} \rfloor$ ,  $T_m(\Lambda) = \Lambda$  and thus the approximation becomes exact fulfilling the condition i).

Condition ii) is also fulfilled.  $T_m(\Lambda)$  indeed preserves all the reduced density matrices consisting of  $m+1$  sites and, as a result, all the expectation values of local operators with support on  $m+1$  consecutive sites. As an example, in the quenches discussed here,  $m \geq 1$  is enough to conserve the energy of the system since the total energy for a transverse field Ising Hamiltonian (4) is the sum of operators with support on only 2 consecutive sites. For a generic Gaussian-fermionic Hamiltonian sum of operators with support on at most  $l$  neighbouring sites, the conservation of the energy is enforced by choosing  $m \geq (l-1)$ . At last the truncation maps translation invariant states to translation invariant states, thus preserving translation invariance for every choice of  $m$ .

We can thus build an approximate time evolution algorithm by approximating  $\Lambda$  with  $T_m(\Lambda)$  at every step of the evolution whose pseudo-code would look like

---

#### Algorithm 1 Truncated time evolution of precision $m$

---

```

1: procedure TRUNC-EVOLV( $\Lambda, N_s, \delta t, m$ )
2:    $t := 0$ 
3:   while  $t < N_s$  do
4:      $\Lambda := T_m(\Lambda)$  ▷ Truncation step
5:      $\Lambda := Evolve(\Lambda, H(\theta_1), \delta t)$  ▷ Evolution step
6:      $t := t + 1$ 
7:   end while
8:   return  $\Lambda$ 
9: end procedure

```

---

Even though the truncation steps preserve the local reduced density matrices of the system they do change the global state. We note, for example, that setting to 0 the out-of-diagonal elements of a matrix modifies its eigenvalues. The actual change can only be found by diagonalising the matrix before and after the truncation. As a result, the approximation can in principle spoil the positivity of the state. We will monitor this specific aspect of the algorithm in the numerical analysis.

Before moving to the numerical results we note that the loss of information due to the truncation of the correlations makes the approximate dynamics not unitary. This is somehow expected. We indeed are trying to obtain a good approximation of the Gaussian diagonal ensemble  $\rho_{GDE(H)}$  whose knowledge, in general, is not sufficient to recover the initial state of the quench. Our approximation renders thus the evolution non-reversible.

In the following we denote by  $\rho(0)$  the density matrix

of the initial state and by  $\rho(t, m)$  its evolution at time  $t$  computed with the truncated time evolution at precision  $m$ . For the maximum value of the precision parameter  $m$   $\rho(t, \lfloor \frac{N}{2} \rfloor) := \rho(t)$ , where  $\rho(t)$  is the exact evolution of the initial density matrix up to time  $t$ .

#### IV. NUMERICAL RESULTS

We start by considering the Hamiltonian (4) with  $N = 100$  sites for the quench  $\theta : \frac{\pi}{4} + 0.1 \rightarrow \frac{\pi}{4} + 0.3$  for an evolution of  $N_s = 6000$  time-steps of length  $\delta t = 0.25$  as a paradigmatic example (the discussion on the dependence of our results on the specific quench scenario are reported in the supplementary material).

Since we are dealing with free fermionic systems the time evolution after the quench can be computed exactly and we can thus compare the results of the approximated algorithm with those obtained during the exact evolution. The approximated algorithm consists in a first step of exact evolution for a time interval  $\delta t$  and a subsequent truncation causing the approximation.

The truncation step erases all the correlations at distance greater than  $m$ , the refinement parameter.

We start by characterising the late-time behaviour of local observables that should be well approximated (at least on average) by their value in the DE [60]. The occupation of a single site  $n := a^\dagger a$  (all sites are equivalent as a consequence of translational invariance) extracted from the approximate dynamics is  $\langle n(t) \rangle_m := \text{Tr}[\rho(t, m)n]$  while its exact value is  $\langle n(t) \rangle := \text{Tr}[\rho(t)n]$  and its value in the diagonal ensemble  $\langle n \rangle_{DE}$ .

The corresponding results are presented in the top panel of Figure 1 where we plot the evolution after the quench of  $\langle n(t) \rangle_m$  versus  $\langle n(t) \rangle$  together with  $\langle n \rangle_{DE}$ . During the exact evolution the expectation value of  $n$  relaxes after moderately long times (of the order  $t/\sin(\theta) = 60$  in Figure 1) to an almost stationary value, well approximated by  $\langle n \rangle_{DE}$ . If the system were infinite this would be the end of the out-of-equilibrium evolution, but due to the finite size of the system, after times of the order of  $N/v$  (where  $v$  is the maximum group velocity of the pseudo particles [11, 32, 39, 45]), the pseudo particles have already travelled through the full system causing return effects and the dynamics to restart.

As expected, the truncation does not affect the dynamics at short time. Since the initial state is the ground state of a gaped Hamiltonian its correlation functions decay exponentially with the distance [2, 3, 10], thus during the initial steps of the evolution  $\langle n(t) \rangle_m$  is extremely close to  $\langle n(t) \rangle$ . As the correlations spread through pseudo particles with a fixed velocity the truncated evolution mimic perfectly the exact one for an interval of time proportional to  $m/v$ . When the correlations spread to distances larger than  $m$ , the approximation induced by the truncation becomes evident displaying, e.g., on shorter time scales larger relaxation times.

In the bottom panel of Figure 1 we repeat the same

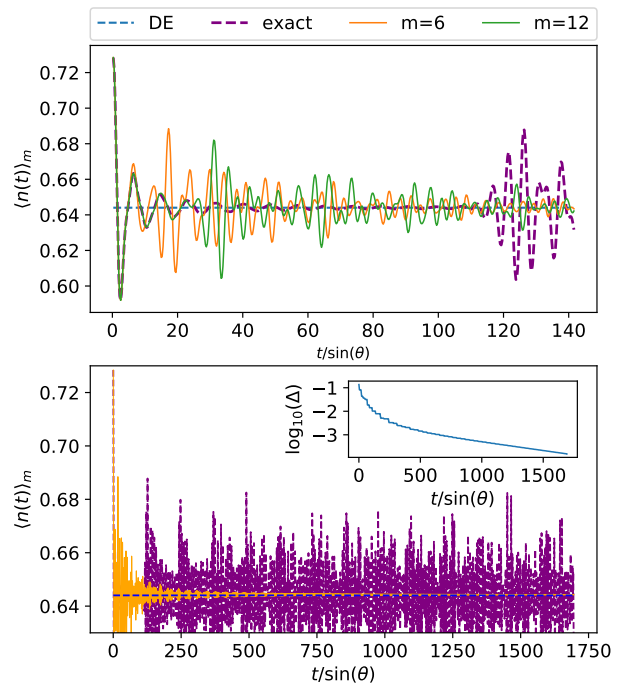


FIG. 1. **(Top)** Evolution after the quench of the expectation value  $n$  in a chain of  $N = 100$  sites for short times. The exact evolution (dashed purple) is plotted together with the results of different truncated evolutions  $\langle n(t) \rangle_m$  with increasing precision parameterised by  $m$  ( $m = 49$  would correspond to the exact evolution). The dashed pale blue line represents the value of  $n$  in the diagonal ensemble  $\langle n \rangle_{DE}$  that should approximate the time average of the expectation value after long times. Focusing on the exact evolution we can appreciate both the relaxation (characterised by damped oscillations around the equilibrium value), and the return effects (e.g. the revival of the oscillations after  $t = 100$ ). The truncated dynamics takes longer to relax than the exact one, as evident by two solid lines representing  $m = 6$  and  $m = 12$ . **(Bottom)** Evolution after the quench of the expectation value  $n$  in a chain of  $N = 100$  sites for long times. The exact long-time dynamics is characterised by relaxation cycles that keeps alternating with the recurrences of the oscillations due to the return effects. The truncated dynamics stabilises around the expectation value  $\langle n \rangle_{DE} := \text{Tr}[\rho_{DE}n]$  that correctly approximate the long-time average of the operator. In the inset indeed we present the amplitude  $\mathcal{A}$  of the envelope of the truncated dynamics showing that it decays very fast towards a small constant value, a finite-size effect that measures the discrepancy between the exact time average and the value attained in the DE.

analysis by considering the evolution for longer times. The value of  $\langle n(t) \rangle_m$  in the truncated dynamics seems to slowly converge to a steady value. In the inset we plot the amplitude  $\mathcal{A}$  of the envelope of the truncated dynamics in logarithmic scale and we see that it quickly reduces but it doesn't reach zero. Indeed as  $m$  increases the truncated evolution resembles more and more the

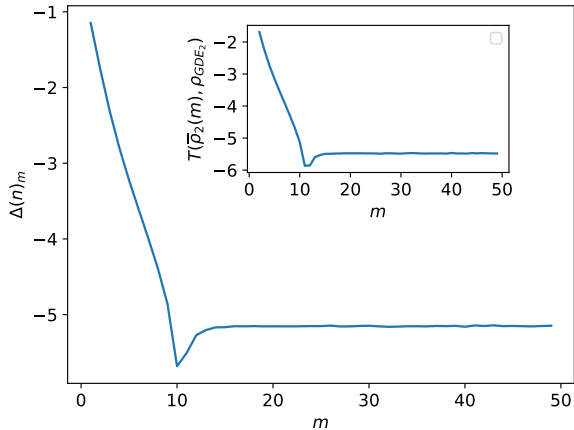


FIG. 2. **(Main)** Difference in logarithmic scale of  $\overline{\langle n \rangle}_m$  and  $\langle n \rangle_{DE}$  as a function of  $m$ . The difference decreases exponentially fast for small  $m$ . For larger  $m$  the envelope of the truncated dynamics is slowly dumped reproducing the exact dynamics, as a consequence of the finite size of the system. At large  $m$ , indeed, the difference oscillates. This allows us to identify an optimal  $m$  (around  $m = 10$  in this case) that provides the best approximation to the DE, more accurate than what obtained with the exact finite size simulation. **(Inset)** The value of the trace distance of the 2-sites reduced density matrix of  $\bar{\rho}$  and  $\rho_{GDE}$ . This quantity presents the same qualitative behaviour than the expectation value of  $\overline{\langle n \rangle}_m$ . We can thus confidently identify the optimal  $m$ , around  $m = 10$  in this case providing the best local approximation to the DE.

exact one and consequently its envelope decay is slower and differs from the DE as a consequence of the finite size of the system.

We now turn to characterising the density matrix  $\bar{\rho}(m)$  associated to the time average of the symbol matrices for each  $m$ ,

$$\bar{\Lambda}(m) = \frac{1}{N_s} \sum_{t=1}^{N_s} \Lambda(t \cdot \delta t, m), \quad (6)$$

in order to quantify how close the truncated evolution equilibrates to the gaussian diagonal ensemble.

The results are presented in Figure 2 where we plot

$$\Delta(n)_m = |Tr[(\bar{\rho}(m) - \rho_{DE})n]|, \quad (7)$$

the difference between the single site occupation on the averaged state and the DE (on the single site the GDE corresponds to the DE).

We note that  $\Delta(n)_m$  decays exponentially for small  $m$  and reaches the minimum at  $m = 10$ . As a result we observe that modest values of  $m$  allow to extract a better local approximation of the DE than what is possible to obtain by performing the exact evolution of the full system. Our approximation indeed allows to filter some of the finite-size effects present in the exact evolution.

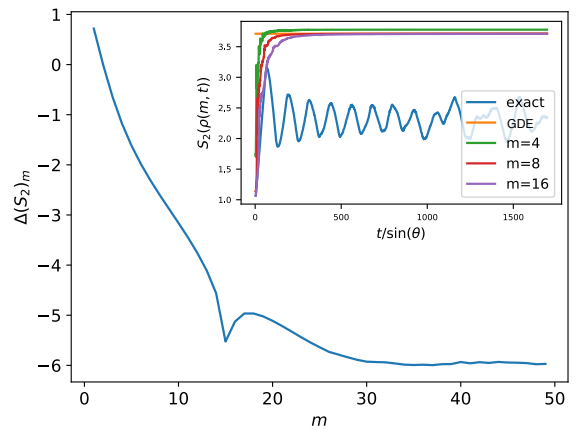


FIG. 3. **(Main)** Difference of  $\bar{S}_2(m)$  with  $S_2(\rho_{GDE})$  in logarithmic scale. The value of  $m$  for the minimum depends on the correlation length of the GDE. **(Inset)** Dynamics of the second Renyi entropies in the truncated dynamics for different precisions. The discrepancy between the exact evolution and the other sets of data could be explained by noticing that in the exact evolution only entanglement contributes to  $S_2$  (the state is always pure), whereas in the other cases classical correlations can also contribute to  $S_2$ . There the states are mixed as a result of the approximation or, in the GDE, by construction.

For bigger values of  $m$ ,  $\Delta(n)_m$  stays constant and eventually increases, as expected, since the exact evolution does not relax exactly to the DE due to finite-size effects.

In the inset we consider the asymptotic value of the trace distance between the matrices  $\bar{\rho}_2(m) = Tr_{[1, \dots, N-2]}[\bar{\rho}(m)]$  and  $\rho_{GDE_2} = Tr_{[1, \dots, N-2]}[\rho_{GDE}]$ .

$$T(\bar{\rho}_2(m), \rho_{GDE_2}) = \frac{\|\bar{\rho}_2(m) - \rho_{GDE_2}\|_{p=1}}{2}. \quad (8)$$

This distance gives a measure of the maximum probability of distinguishing between two states with an optimal measurement. The behaviour of this quantity is similar to the one of  $\Delta(n)_m$ , thus we can see that  $\bar{\rho}(m)$  is a good local approximation for the DE.

The truncated evolution thus provides a good approximation of the local properties of the DE. We thus need to understand how close the global matrix obtained from the truncated algorithm is to the GDE. The first observation is that the purity of  $\rho(t, m)$  decreases during the evolution, thus the truncation step of the algorithm adds mixedness to the system.

In the inset of figure 3, we analyse the second Renyi entropy of half-chain  $S_2 = -\log(Tr[\rho_{N/2}(t, m)^2])$ , showing that for any  $m$  it increases as a function of time.

In the main plot we consider the deviation of the average of  $S_2$  for half chain with respect to its gaussian diagonal ensemble value.

$$\Delta(S_2)_m = |S_2(\bar{\rho}(m)) - \rho_{GDE}|. \quad (9)$$

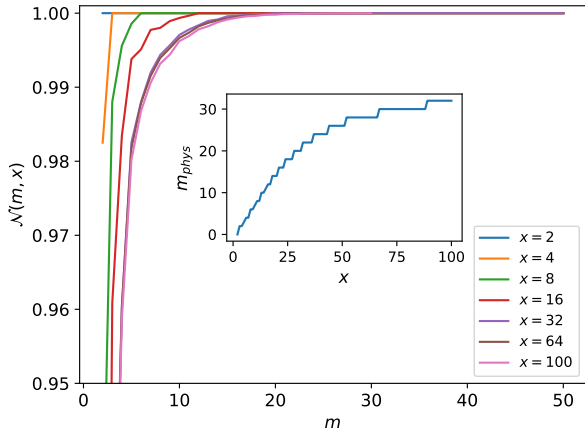


FIG. 4. **(Main)** The value of  $\mathcal{N}(m, x)$  versus  $m$  is plotted for different dimensions  $x$  of the reduced matrix  $\bar{\rho}(m)_x$ . When  $\mathcal{N}(m, x) = 1$  then  $\bar{\rho}(m)_x$  is physical. **(Inset)** Minimum value of the precision  $m_{phys}$  required for a specific  $x$  such that  $\bar{\rho}(m)_x$  is physical. It is remarkable that already for moderate values of  $m$  the approximate state is physical over a large range of distances.

We have that at  $m = 14$   $\Delta(S_2)_m$  has the first minimum. Differently from  $\Delta(n)_m, \Delta(S_2)_m$  decays again before reaching a steady value.

Despite the fact that both local and global properties of the truncated evolution approach those of the GDE, in order to assert that  $\bar{\rho}(m)$  is a good approximation of the GDE we need to check that it is a physical state. This point has been completely ignored in the literature due to the exponential complexity of the task. Here again free fermions help addressing this issue with only polynomial resources.

A matrix is a density matrix only if it is positive semi-definite. Checking if a matrix is positive requires diagonalising it, and since the size of the matrix increases exponentially with the size of the system this becomes unfeasible for very small systems. In the case of tensor networks, the task is shown to be NP-hard in the dimension of the system [61].

Conversely the symbol matrix  $\Lambda$  of a free-fermionic system represents a physical state if its eigenvalues are in the interval  $[0, 1]$  [58]. In order to check this property we just need to diagonalise the symbol matrix, an operation that scales polynomially with the system size. The eigenvalues of  $\Lambda$  appear in couples  $(\lambda_i, 1 - \lambda_i)$ .  $\Lambda$  is non-physical if it contains at least one eigenvalue smaller than 0 (hence its partner will be larger than 1).

We thus define the quantity  $\mathcal{N}(m, x)$ , that is 1 minus the sum of the negative eigenvalues of  $\Lambda(m)_x$ ,

$$\mathcal{N}(x, m) = 1 - \frac{\|\Lambda(m)_x\|_{l=1} - 1}{2} = 1 - \sum_i \frac{|\lambda_i| - \lambda_i}{2}, \quad (10)$$

where  $\Lambda(m)_x$  is the symbol matrix of  $Tr_{[1, \dots, N-x]}[\bar{\rho}(m)] = \bar{\rho}(m)_x$  and  $\{\lambda_i\}_i$  are the eigenvalues of  $\Lambda(m)_x$ .

$\mathcal{N}(m, x) = 1$  for a physical  $\bar{\rho}(m)_x$ , since as mentioned all the eigenvalue are in this case positive in the interval between 0 and 1.  $\mathcal{N}(m, x) = 1$  decreases as the sum of negative eigenvalues of  $\Lambda(m)_x$  decreases.

In Figure 4 we plot  $\mathcal{N}(m, x)$  versus  $m$  for different values of  $x$ . We can see that for large enough  $m$  the reduced density matrices of  $\bar{\rho}(m)$  become physical for every chosen size  $x$ . In the inset, we plot the minimum value of precision  $m_{phys}$  required for  $\bar{\rho}(m)_x$  to be physical for every choice of its size  $x$ . Interestingly, we see that for  $x \leq 16$  the value of  $m$  necessary to represent a physical state is similar to the optimal  $m$  identified previously.

This fact should be related to the finite correlation length present in the GDE. In order to describe correctly the expectation value of a local operator we just need to embed the local system into a larger system whose size exceed the correlation length of the desired state (see e.g. [62–66]).

## V. CONCLUSION

We have identified some robust aspects of the out-of-equilibrium dynamics encoded in the late-time expectation value of local operators after the quench. By exploiting this robustness we have designed an approximate algorithm that allows to predict the relaxed values of local operators with limited computational resources.

The key idea underlying the design of our algorithm, is to protect, from the approximations, the relevant conserved quantities. These are defined as the conserved quantities built out of local densities. The degree of locality of such conserved quantities naturally acts as the refinement parameter of the algorithm allowing to increase the precision of the results by increasing the computational cost.

We have benchmarked the algorithm in the case of free-fermionic systems and observed that for modest values of the refinement parameter the results are in good agreement with the exact ones. Furthermore their precision improves exponentially as we increase the computational resources.

In particular we have identified the lower value of the refinement parameter that guarantees the physicality of the approximate states generated by the algorithm. We have observed that, in most cases, for moderate values of the refinement parameter  $m$ , our approximate algorithm provides a better local approximation to the DE than what can be obtained by performing the exponentially expensive exact evolution of the finite-size system over much longer times.

The next step is to check if the same picture holds in the presence of strong interactions both in the integrable and non integrable scenarios. It would also be interesting to compare and relate this approach with the existing

complementary one proposed in [17, 26, 56, 67–70].

We acknowledge the discussion on the topic with Frank Verstraete, Marie Carmen Banuls, Frank Pollman. JS was supported by the doctoral training partnership (DTP 2016-2017) of the University of Strathclyde.

## VI. APPENDIX

### A. Fermionic Gaussian Systems

The generic quadratic Fermionic Hamiltonian on  $N$  sites can be written as

$$H = \frac{1}{2} \sum_{i,j=0}^{N-1} \left[ A_{i,j} a_i^\dagger a_j - \bar{A}_{i,j} a_i a_j^\dagger + B_{i,j} a_i a_j - \bar{B}_{i,j} a_i^\dagger a_j^\dagger \right] \quad (11)$$

where  $A_{i,j}, B_{i,j} \in \mathbb{C}$ ,  $A = A^\dagger$ ,  $B^T = -B$  and the annihilation and creation operators  $a_i$  and  $a_i^\dagger$  obey the anticommutation relations  $\{a_i^\dagger, a_j\} = \delta_{i,j}$ ,  $\{a_i^\dagger, a_j^\dagger\} = \{a_i, a_j\} = 0$ .

In the main text we restricted to the single parameter Hamiltonian  $H(\theta)$  defined by the matrices

$$\begin{aligned} A(\theta)_{i,j} &= -f_{N,i,j} \sin(\theta) (\delta_{i+1,j} + \delta_{i,j+1}) - 2 \cos(\theta) \delta_{i,i}, \\ B(\theta)_{i,j} &= f_{N,i,j} \sin(\theta) (\delta_{i+1,j} - \delta_{i,j+1}), \end{aligned} \quad (12)$$

with the term

$$f_{N,i,j} = \begin{cases} -(-1)^{(N)}, & \text{if } i \vee j = N \\ 1, & \text{otherwise,} \end{cases} \quad (13)$$

necessary for the antisymmetrisation with periodic boundary condition.

This one parameter Hamiltonian is the mapping to fermions of the 1D transverse field Ising model on  $N$  sites and periodic boundary condition

$$H(\theta) = -\sin(\theta) \sum_{i=0}^{N-1} \sigma_i^x \sigma_{i+1}^x - \cos(\theta) \sum_{i=0}^{N-1} \sigma_i^z, \quad (14)$$

where  $(\sigma_i^x, \sigma_i^y, \sigma_i^z)$  are the Pauli matrices on site  $i$ ,  $\theta \in [0, \frac{\pi}{2}]$  and  $N$  is the number of sites[71].

A Fermionic Gaussian state is a ground or thermal state of a quadratic Fermionic Hamiltonian. Using Wick's theorem it is possible to show that Gaussian states are completely characterised by the collection of their 2–points correlators

$$\Lambda_{i,j}^{TL} = \text{Tr} \left[ \rho a_i^\dagger a_j \right] \quad (15)$$

$$\Lambda_{i,j}^{TR} = \text{Tr} \left[ \rho a_i^\dagger a_j^\dagger \right], \quad (16)$$

where the correlators  $\text{Tr} \left[ \rho a_i^\dagger a_j \right]$  and  $\text{Tr} \left[ \rho a_i^\dagger a_j^\dagger \right]$  are said to be a correlators at distance  $d_{i,j}$ , where

$d_{i,j} \equiv \min(|i-j|, |N-(i-j)|)$ . We have that  $\Lambda^{TL}$  is Hermitian and  $\Lambda^{BL}$  is skew-symmetric. The 2–points correlators can be arranged in the block matrix

$$\Lambda = \left[ \begin{array}{c|c} \Lambda^{TL} & \Lambda^{TR} \\ \hline -\Lambda^{TR*} & \mathbb{I} - \Lambda^{TLT} \end{array} \right],$$

called the symbol matrix [57]. The symbol matrix is hermitian and for any admissible symbol matrix of a physical fermionic system, the eigenvalues have to be in the interval  $[0, 1]$ .

The 2–points correlators of translational invariant states depend only on the distance, thus the elements  $\Lambda_{i,j}^{TL}$  simplify to elements of the circulant matrices  $\Lambda_{d_{i,j}}^{TL}$  which depend only on the distance between the indices.

The space of Gaussian states is closed under evolution induced by quadratic Hamiltonians, thus, if we start with a Gaussian state and evolve it with an Hamiltonian of the form (11) the knowledge of  $\Gamma^A$  at any time would completely characterise the state of the system.

The reduced state over a set of sites  $S$  is still a Gaussian and is characterised by the symbol matrix of all the 2–points correlators with support on  $S$ .

### B. Numerical results for different quenches

In this section we represent the plots of the main part obtained from the dynamics with 2 different quenches. In particular we choose

$$\text{Quench } A: \quad \theta: \frac{\pi}{4} + 0.1 \quad \rightarrow \quad \frac{\pi}{4} + 0.4 \quad (17)$$

$$\text{Quench } B: \quad \theta: \frac{\pi}{4} + 0.25 \quad \rightarrow \quad \frac{\pi}{4} + 0.4. \quad (18)$$

For both quenches the dynamics is generated by the same Hamiltonian but the initial state is different in temperature. From figures 5 and 6 we note that the precision  $m$  for the best local approximation is proportional to the final correlation length of the quench.

From figures 7 and 8 we note again that the precision  $m$  for the first negative spike is proportional to the final correlation length of the quench. For the quench  $B$ , after the first spike, the precision return to increase for larger  $m$ .

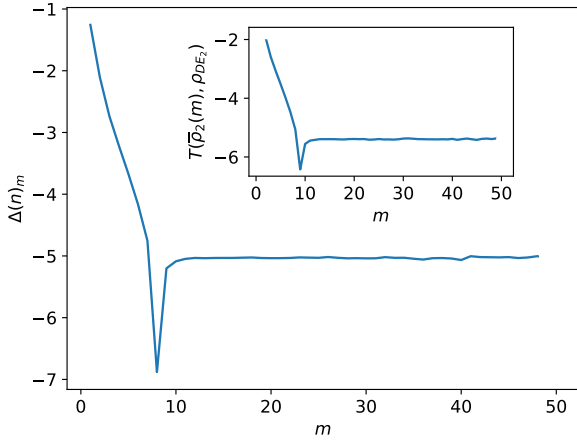


FIG. 5. [Quench A] (Main) Difference in logarithmic scale of  $\langle n \rangle_m$  with  $\langle n \rangle_{DE}$ . We note the fast convergence with  $m$ . For bigger  $m$  the envelope of the truncated dynamics shrinks slowly, for this reason at big values of  $m$  the difference oscillate. (Inset) The value of the trace distance of the 2-sites reduced density matrix of  $\bar{\rho}$  and  $\rho_{GDE}$ . This allows us to identify the optimal  $m$  providing the best local approximation to the DE.

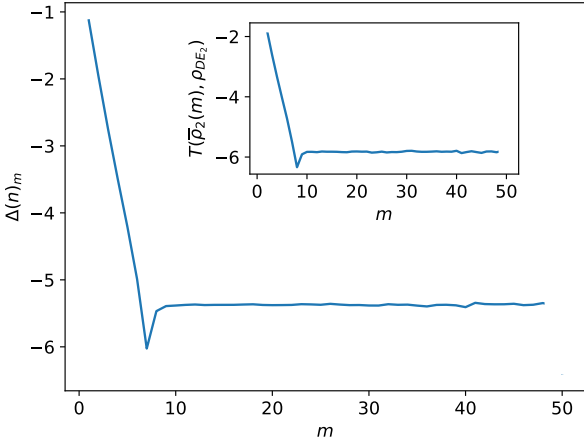


FIG. 6. [Quench B] (Main) Difference in logarithmic scale of  $\langle n \rangle_m$  with  $\langle n \rangle_{DE}$ . We note the fast convergence with  $m$ . For bigger  $m$  the envelope of the truncated dynamics shrinks slowly, for this reason at big values of  $m$  the difference oscillate. (Inset) The value of the trace distance of the 2-sites reduced density matrix of  $\bar{\rho}$  and  $\rho_{GDE}$ . This allows us to identify the optimal  $m$  providing the best local approximation to the DE.

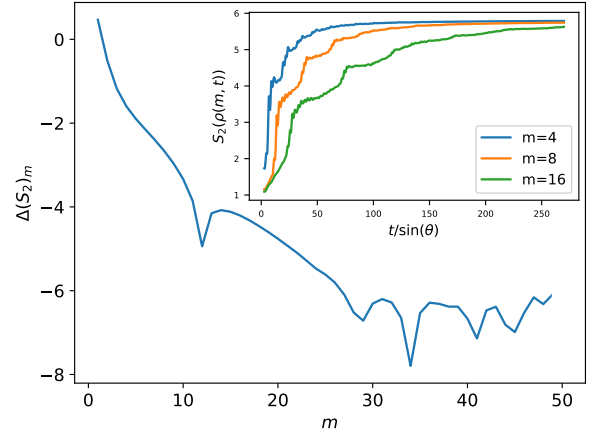


FIG. 7. [Quench A] (Main) Difference of  $\bar{S}_2(m)$  with  $S_2(\rho_{GDE})$  in logarithmic scale. (Inset) Dynamics of the second Renyi entropies in the truncated dynamics for different precisions.

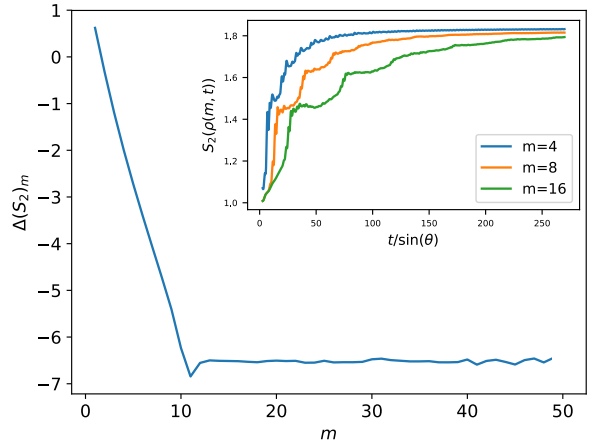


FIG. 8. [Quench B] (Main) Difference of  $\bar{S}_2(m)$  with  $S_2(\rho_{GDE})$  in logarithmic scale. (Inset) Dynamics of the second Renyi entropies in the truncated dynamics for different precisions.



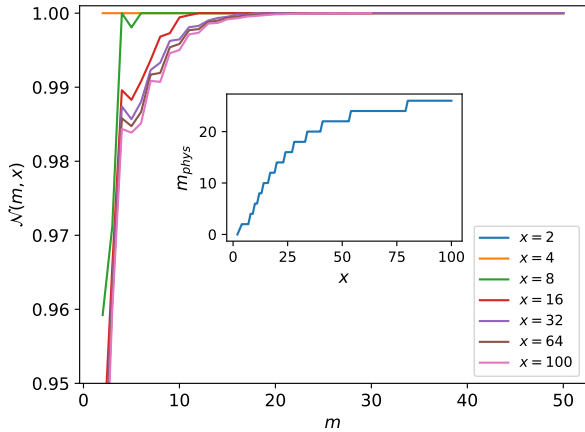


FIG. 9. [Quench A](Main) The value of  $\mathcal{N}(m, x)$  versus  $m$  is plotted for different dimensions  $x$  of the reduced matrix  $\bar{\rho}(m)_x$ . When  $\mathcal{N}(m, x) = 1$  then  $\bar{\rho}(m)_x$  is physical. (Inset) Minimum value of the precision  $m_{phys}$  for a specific  $x$  such that  $\bar{\rho}(m)_x$  is physical.

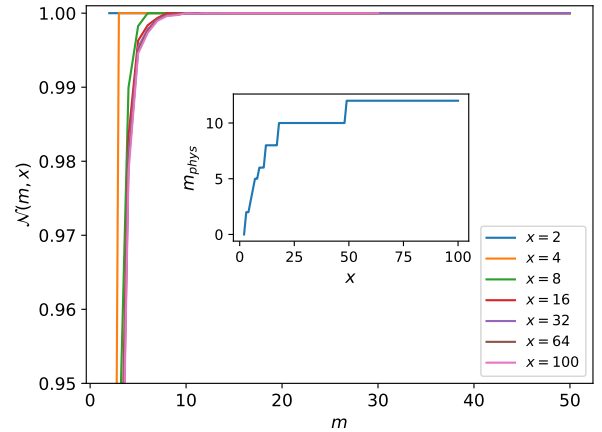


FIG. 10. [Quench B](Main) The value of  $\mathcal{N}(m, x)$  versus  $m$  is plotted for different dimensions  $x$  of the reduced matrix  $\bar{\rho}(m)_x$ . When  $\mathcal{N}(m, x) = 1$  then  $\bar{\rho}(m)_x$  is physical. (Inset) Minimum value of the precision  $m_{phys}$  for a specific  $x$  such that  $\bar{\rho}(m)_x$  is physical.

From figures 9 and 10 we note that the minimum precision  $m_{phys}$  for the physicality of the whole system is again proportional to the correlation length after the quench. For shorter correlation length a small value of the precision  $m$  is sufficient in order to obtain a globally physical states that locally well approximate the diagonal ensemble.

- 
- [1] G. Parisi, *Statistical Field Theory* (Addison-Wesley, 1988).
- [2] M. B. Hastings, *J. Stat. Mech.* **2007**, P08024 (2007).
- [3] M. M. Wolf, F. Verstraete, M. B. Hastings, and J. I. Cirac, *Physical Review Letters* **100** (2008).
- [4] J. Eisert, M. Cramer, and M. B. Plenio, *Rev. Mod. Phys.* **82**, 277 (2010).
- [5] S. R. White, *Physical Review B* **48**, 10345 (1993).
- [6] S. R. White, *Physical Review Letters* **69**, 2863 (1992).
- [7] R. Orús, *Annals of Physics* **349**, 117 (2014).
- [8] U. Schollwöck, *Annals of Physics* **326**, 96 (2011).
- [9] G. Vidal, *Physical Review Letters* **91**, 147902 (2003).
- [10] J. Eisert, *Modeling and Simulation* **3**, 39 (2013).
- [11] P. Calabrese and J. Cardy, *J. Stat. Mech.* **2005**, P04010 (2005).
- [12] G. D. Chiara, S. Montangero, P. Calabrese, and R. Fazio, *J. Stat. Mech.* **2006**, P03001 (2006).
- [13] A. M. Läuchli and C. Kollath, *J. Stat. Mech.* **2008**, P05018 (2008).
- [14] H. Kim and D. A. Huse, *Phys. Rev. Lett.* **111**, 127205 (2013).
- [15] M. Fagotti and M. Collura, arXiv:1507.02678 [cond-mat, physics:math-ph, physics:quant-ph] (2015), arXiv:1507.02678 [cond-mat, physics:math-ph, physics:quant-ph].
- [16] M. Kormos, M. Collura, G. Takács, and P. Calabrese, *Nature Physics* **13**, 246 (2017).
- [17] C. W. von Keyserlingk, T. Rakovszky, F. Pollmann, and S. L. Sondhi, *Phys. Rev. X* **8**, 021013 (2018).
- [18] M. Collura, M. Kormos, and G. Takacs, arXiv:1801.05817 [cond-mat] (2018), arXiv:1801.05817 [cond-mat].
- [19] S. Trotzky, Y.-A. Chen, A. Flesch, I. P. McCulloch, U. Schollwöck, J. Eisert, and I. Bloch, *Nat Phys* **8**, 325 (2012).
- [20] J. M. Deutsch, *Physical Review A* **43**, 2046 (1991).
- [21] M. Srednicki, *Physical Review E* **50**, 888 (1994).
- [22] M. Rigol, V. Dunjko, and M. Olshanii, *Nature* **452**, 854 (2008).
- [23] M. Rigol and M. Srednicki, *Phys. Rev. Lett.* **108**, 110601 (2012).
- [24] L. D'Alessio, Y. Kafri, A. Polkovnikov, and M. Rigol, *Advances in Physics* **65**, 239 (2016), arXiv:1509.06411.
- [25] M. Rigol, *Phys. Rev. Lett.* **112**, 170601 (2014).
- [26] C. D. White, M. Zaletel, R. S. K. Mong, and G. Refael, (2017).
- [27] J. Hauschild, E. Leviatan, J. H. Bardarson, E. Altman, M. P. Zaletel, and F. Pollmann, (2017).
- [28] M. Rigol, V. Dunjko, V. Yurovsky, and M. Olshanii, *Physical Review Letters* **98**, 050405 (2007).
- [29] M. Cramer, C. M. Dawson, J. Eisert, and T. J. Osborne, *Phys. Rev. Lett.* **100**, 030602 (2008).

- [30] T. Barthel and U. Schollwöck, *Phys. Rev. Lett.* **100**, 100601 (2008).
- [31] M. Cramer and J. Eisert, *New J. Phys.* **12**, 055020 (2010).
- [32] P. Calabrese, F. H. Essler, and M. Fagotti, *Journal of Statistical Mechanics: Theory and Experiment* **2012** (2012).
- [33] T. Langen, S. Erne, R. Geiger, B. Rauer, T. Schweigler, M. Kuhnert, W. Rohringer, I. E. Mazets, T. Gasenzer, and J. Schmiedmayer, *Science* **348**, 207 (2015).
- [34] E. Ilievski, J. De Nardis, B. Wouters, J.-S. Caux, F. H. L. Essler, and T. Prosen, *Phys. Rev. Lett.* **115**, 157201 (2015).
- [35] L. Vidmar and M. Rigol, *J. Stat. Mech.* **2016**, 064007 (2016).
- [36] M. Fagotti and F. H. L. Essler, *Physical Review B - Condensed Matter and Materials Physics* **87** (2013).
- [37] F. H. Essler, G. Mussardo, and M. Panfil, *Journal of Statistical Mechanics: Theory and Experiment* **2017** (2017).
- [38] L. Vidmar and M. Rigol, *Journal of Statistical Mechanics: Theory and Experiment* **2016** (2016).
- [39] P. Calabrese, F. H. Essler, and M. Fagotti, *Physical Review Letters* **106** (2011).
- [40] J. Surace, In preparation.
- [41] C. Murthy and M. Srednicki, arXiv:1809.03681 [cond-mat] (2018), arXiv:1809.03681 [cond-mat].
- [42] M. Gluza, J. Eisert, and T. Farrelly, arXiv:1809.08268 [cond-mat, physics:quant-ph] (2018), arXiv:1809.08268 [cond-mat, physics:quant-ph].
- [43] A. Polkovnikov, K. Sengupta, A. Silva, and M. Vengalattore, *Rev. Mod. Phys.* **83**, 863 (2011).
- [44] V. Alba and P. Calabrese, *PNAS* **114**, 7947 (2017).
- [45] P. Calabrese, F. H. Essler, and M. Fagotti, *Journal of Statistical Mechanics: Theory and Experiment* **2012** (2012).
- [46] F. Verstraete, J. J. García-Ripoll, and J. I. Cirac, *Phys. Rev. Lett.* **93**, 207204 (2004).
- [47] Here we consider only systems whose excitations are extended and can be described using pseudo particles. A treatment of different systems such as those described in [72] will be performed separately.
- [48] For a detailed analysis of the universal aspects encoded in the light cone spreading of the correlations after a quench we refer the reader to Ref. [73].
- [49] B. Pozsgay, M. Mestyán, M. A. Werner, M. Kormos, G. Zaránd, and G. Takács, *Phys. Rev. Lett.* **113**, 117203 (2014).
- [50] V. Alba, *Physical Review B - Condensed Matter and Materials Physics* **91** (2015), 10.1103/PhysRevB.91.155123.
- [51] M. Kollar and M. Eckstein, *Physical Review A* **78** (2008), 10.1103/PhysRevA.78.013626.
- [52] D. M. Gangardt and M. Pustilnik, *Phys. Rev. A* **77**, 041604 (2008).
- [53] E. T. Jaynes, *Physical Review* **106**, 620 (1957).
- [54] E. T. Jaynes, *Physical Review* **108**, 171 (1957).
- [55] M. Perarnau-Llobet, A. Riera, R. Gallego, H. Wilming, and J. Eisert, *New Journal of Physics* **18** (2016).
- [56] E. Leviatan, F. Pollmann, J. H. Bardarson, D. A. Huse, and E. Altman, (2017).
- [57] E. Greplová, Master Thesis (2013).
- [58] C. V. Kraus, PhD. Thesis.
- [59] T. D. SCHULTZ, D. C. MATTIS, and E. H. LIEB, *Rev. Mod. Phys.* **36**, 856 (1964).
- [60] M. Rigol, *Physical Review A - Atomic, Molecular, and Optical Physics* **80** (2009).
- [61] M. Kliesch, D. Gross, and J. Eisert, *Physical Review Letters* **113**, 160503 (2014).
- [62] S. Hernández-Santana, A. Riera, K. V. Hovhannisyán, M. Perarnau-Llobet, L. Tagliacozzo, and A. Acín, *New Journal of Physics* **17** (2015).
- [63] M. Kliesch, C. Gogolin, M. J. Kastoryano, A. Riera, and J. Eisert, *Phys. Rev. X* **4**, 031019 (2014).
- [64] A. D. Pasquale, D. Rossini, R. Fazio, and V. Giovannetti, *Nature Communications* **7**, 12782 (2016).
- [65] A. García-Saez, A. Ferraro, and A. Acín, *Phys. Rev. A* **79**, 052340 (2009).
- [66] A. Ferraro, A. García-Saez, and A. Acín, *EPL* **98**, 10009 (2012).
- [67] J. Wurtz and A. Polkovnikov, arXiv:1808.08977 [cond-mat.stat-mech] (2018), arXiv:1808.08977 [cond-mat.stat-mech].
- [68] J.-S. Caux and F. H. L. Essler, *Phys. Rev. Lett.* **110**, 257203 (2013).
- [69] J. D. Nardis, L. Piroli, and J.-S. Caux, *J. Phys. A: Math. Theor.* **48**, 43FT01 (2015).
- [70] J.-S. Caux, *J. Stat. Mech.* **2016**, 064006 (2016).
- [71] A. Dutta, U. Divakaran, S. Diptiman, B. K. Chakrabarti, T. F. Rosenbaum, and G. Aeppli, arXiv:1012.0653 (2012).
- [72] A. Nahum, J. Ruhman, S. Vijay, and J. Haah, *Phys. Rev. X* **7**, 031016 (2017).
- [73] L. Cevolani, J. Despres, G. Carleo, L. Tagliacozzo, and L. Sanchez-Palencia, *Phys. Rev. B* **98**, 024302 (2018).